Wood Science and Technology (2024) 58:135–160
https://doi.org/10.1007/s00226-023-01508-z

ORIGINAL

Wood-water interactions of primers to enhance wood-polyurethane bonding performance

Thomas Böger[1] · Max Engelhardt[1] · Francis Tangwa Suh[2] · Klaus Richter[1] · Antoni Sanchez-Ferrer[1]

Received: 9 August 2023 / Accepted: 2 November 2023 / Published online: 23 November 2023

Abstract

Today, using one-component polyurethane (1c-PUR) adhesives in the manufacturing of engineered wood products from spruce is common practice. However, the use of other wood species can require the application of a primer to fulfill normative requirements. Previous research shows the primers' effectiveness, especially in moist environments. However, the primers' exact mode of action remains not yet fully understood. We hypothesize a reduction in the hygroscopic behavior of the primer-treated wood—intensity and kinetics—that could reduce the formation of stresses in the bond line region. To test this hypothesis, two commercially available primers, based on Polysorbate 20 and poly(ethylene glycol), and the hydroxymethylated resorcinol (HMR) primer are examined with wood from beech, birch, larch, and Douglas fir. Swelling experiments show that of each primer a portion infiltrates and swells the wood cell walls, affecting the wood's hygroscopic and mechanical properties. In stepwise sorption experiments, it is seen that the primers influence differently the amount of moisture uptaken by the wood (adsorption). The rate at which the moisture spreads within the wood (diffusivity) also changed differently for the primers, while the rate at which the moisture moves through the wood (permeability) remains unchanged. The application of all primers improves the bulk flow behavior and thus the void penetration of the adhesive into the lumina in the interphase region, which in turn leads to a reduced bond line thickness. All three primers improve the tensile shear strength. The hygroscopic changes caused by the primers appear too small to be claimed as the sole and primary cause of their functionality, whereas more relevance is seen in the primers' cell wall infiltration and the increased adhesive's void penetration.

Extended author information available on the last page of the article

Introduction

In the field of adhesion technology, a primer is defined as *"a coating applied to a surface, prior to the application of an adhesive to improve the performance of the bond"* (ASTM D 907 2015). The use of primers is a common practice for bonding various materials, e.g., metals, ceramics, polymers, or tooth enamel (Ebnesajjad 2011; Rasche 2012), while the use of a primer is rare when bonding solid wood. The only major application is the production of engineered wood products (EWP), i.e., glued laminated (GLT) or cross-laminated timber (CLT), with one-component polyurethane adhesive (1c-PUR) in combination with certain wood species. These are species with high extractive content, e.g., larch and yellow-cedar (Cheng et al. 2010; Okkonen et al. 1998), or with high strength properties, especially hardwoods, e.g., beech, ash and birch. Without the use of a primer, commercial 1c-PUR adhesives in combination with these wood species risk to not reliably fulfilling the complete set of building and safety standards defined for structural wood bonding, e.g., EN 15425 (2017), CSA O112.9-10 (2014) and ASTM D 2559 (2004). An overview of primer types used for solid wood bonding is given by Böger et al. (2022). A technical alternative to the use of 1c-PUR adhesives with primers is the use of water-based, two-component adhesives, i.e., melamine–urea–formaldehyde (MUF), phenol–resorcinol–formaldehyde (PRF) or emulsion-polymer isocyanate (EPI). However, together with the need for mixing the two components and a limited pot life, those adhesive types also require longer cycle times.

The hydroxymethylated resorcinol (HMR) primer is an aqueous resorcinol–formaldehyde solution, which is applied to the wood surface while still reactive, with an average molar mass of a cured repeating unit of 128 g/mol, corresponding to a number of sorption sites of 15.6 mmol/g. The HMR primer was developed in the USDA Forest Products Laboratory (Madison WI, USA) and introduced in 1995. Vick et al. (1995) originally explained the functionality of the HMR primer to be a coupling agent assisting both, the adhesive and the wood, for better chemical bonding. Later, a simplification of the HMR primer's application was achieved by Christiansen et al. (2000), by introducing a novolac-like version of the HMR, the n-HMR, which could be stored until its use. Gardner et al. (2005) and Christiansen (2005) questioned the previously assumed coupling effects to be primarily responsible for the positive effects of the HMR primer. Today, the HMR's mode of action is attributed to two modifications of the wood that flanks the bond line: (i) a thin, hydrophobic coating on the cell wall surfaces (Böger et al. 2022), and (ii) an interphase of primer infiltrated cell walls with modified properties that allow for a more beneficial stress transfer with adhesives, which are incapable of infiltrating the cell walls (Frihart 2009). Since its introduction in 1995, extensive work has been conducted by numerous authors, which is consolidated in the review by Böger et al. (2022). This review emphasizes that the effects of this modification on the interactions of HMR-treated wood with water are not sufficiently understood. A reduction in the hygroscopic behavior of the primer-treated wood—intensity and kinetics—could reduce the formation of stresses in the bond line region.

The adhesive producer Henkel & Cie. AG (Sempach Station, Switzerland) offers two commercially available primer systems in combination with their 1c-PUR adhesives. The first primer system is based on poly(ethylene glycol) (PEG), a chain molecule consisting of repeating ether units with hydroxyl groups at both ends. The average molar mass of the hydrophilic PEG in this primer is around 600 g/mol, which corresponds to a number of sorption sites of 3.3 mmol/g. The PEG-based primer is commercially available under the trade name LOCTITE® PR 7010 PURBOND and is covered under the European patent No. 2 848 638 (Amen-Chen et al. 2020). According to Henkel, the primer is designed for larch wood, as well as other wood species with a high content of extractives (Henkel & Cie. AG 2015c, 2017). Lehringer et al. (2014) showed the effectiveness of the primer in combination with larch wood in terms of improved delamination resistance.

The second primer system from Henkel is based on Polysorbate 20 (PS20), which consists of a sorbitan core, where three of its four hydroxyl groups are substituted by OH-terminated short PEG chains with a total amount of repeating units of 20, and once by a fatty acid. This structure results in amphiphilic properties of the molecule. The average molar mass of the PS20 is 1228 g/mol, which corresponds to a number of sorption sites of 2.4 mmol/g. The primer is commercially available under the trade name LOCTITE® PR 3105 PURBOND and is covered under U.S. patent No. 9,649,826 (Swiezkowski et al. 2017). According to its technical data sheet (TDS) and application guides, the primer can be used with different wood species, i.e., beech and Douglas fir (Henkel & Cie. AG 2015a, b, 2018). Different publications show the primer's effectiveness with various wood species by directly comparing the bond performance with and without primer, i.e., for beech (Bockel et al. 2020; Lehringer et al. 2014), Douglas fir, southern yellow pine (Amen-Chen et al. 2015), ash, beech, oak (Luedtke et al. 2015) and ash (Clerc et al. 2018). In addition, Konnerth et al. (2016) bond ash, beech, birch, hornbeam, oak, poplar, and black locust, with the PS20-based primer, unfortunately, without comparing the results to untreated wood. Concerning the functionality of the PS20-based primer, atomic force microscopy and Raman spectroscopy imaging by Casdorff et al. (2018) suggest an infiltration of the PS20 into the wood cell walls, as well as some portion of PS20 to remain on the interface of the S3 cell wall and the lumen. According to Clerc et al. (2018), the effectiveness of the PS20-based primer does not just depend on the quantity of pure PS20 applied but also on the concentration of its aqueous solution. Bockel et al. (2020) show that the treatment with PS20 promotes a reduction in the accessible hydroxyl groups (based on sorption measurements) and a reduction in Young's modulus and hardness (based on nanoindentation).

The available first results with the HMR primer and PS20-based primer and the absence of research concerning the PEG-based primer motivated the present research. So far, there exists no comparative research on the three wood primer types. Therefore, the objective of the following research is to assess the primers' interactions with wood and water and the influence of these interactions on the primers' effects on 1c-PUR bonding. Our research aims to contribute to the understanding of the functionality of the three primers and, in perspective, ease the possible integration of the primers' mode of action into adhesive systems. We hypothesize that the wood-moisture relationships during the application of the primers and their

effects on the diffusion and permeability coefficients are important and contribute decisively to the mode of action. We support the hypothesis that the reactive HMR primer forms covalent bonds with the wood's polymers introduced by Vick et al. (1995), while the primers based on PS20 and PEG, do not form covalent bonds and remain water-solvable after their application. We therefore carry out moisture physics, swelling and leach out, adhesive void penetration and shear strength experiments to prove this.

Materials and methods

Wood samples

Four different wood species were used within the present study: (i) European beech (*Fagus sylvatica* L.) from Baden-Württemberg (Germany), (ii) Silver birch (*Betula pendula* Roth) from Lieksa (Finland), (iii) European larch (*Larix decidua* Mill.) from Styria (Austria), and (iv) Douglas fir (*Pseudotsuga menziesii* (Mirbel) Franco) from Rhineland-Palatinate (Germany). The experiments presented were all conducted by default on beech wood. However, sorption and tensile shear strength experiments were also conducted with the other wood species, whose results are presented in the supplementary information (SI). Before specimen preparation, boards of $120 \times 20 \times 4$ cm^3 (l × w × h) were seasoned at 20 ± 1 °C and 65 ± 3%.

Primer systems and their application

In this study, the 'novolak' version of the HMR primer was used, where formaldehyde is added in two stages, following the formulation of Christiansen et al. (2003). The reactive components (resorcinol and formaldehyde) of the primer were dissolved in approx. 95% (w/w) of water.

The PS20-based primer was obtained from Henkel & Cie. AG as a concentrate, containing 100% of the active substance, according to its TDS (Henkel & Cie. AG 2018). For its application, the concentrate was diluted with water to a 10% solution.

The PEG-based primer was obtained from Henkel & Cie. AG as a ready-to-use aqueous solution with 15% active material, according to its TDS (Henkel & Cie. AG 2017).

Swelling and leach-out experiments

To observe the swelling caused by the primer application, beech wood disks were sampled from a single wood piece of approx. $4 \times 2 \times 2$ cm^3 (t × r × l). Slices containing the same year rings, with a radial longitudinal surface and a thickness of approx. 300 µm were obtained using a sledge microtome. From these slices, circular specimens of 11 mm diameter were obtained using a sharp puncher. The specimen preparation and the entire testing were carried out in an air-conditioned laboratory at 20 ± 1 °C and 65 ± 3% RH.

Before the primer was applied, the specimens were exposed to water to let compressed fibers from the mechanical preparation swell and rise, and to relax possible stresses, to avoid the resulting increase of thickness being falsely attributed to the effect of the primers' active substances. Therefore, the specimens were dipped into deionized water for 10 s and reconditioned until they reached a constant mass before determining their mass and thickness. This procedure was carried out three times, with around one week between each iteration. After the second and third cycle, no further changes in mass and thickness were observed. The measured values after the third cycle were considered the wood's mass (m_w) and thickness (t_w) reference values without primer. The mass of the specimens was measured with 0.01 mg resolution using an analytical balance 1712MP8 from Sartorius (Göttingen, Germany). The thickness was measured in a stationary length gage MT101M from Johannes Heidenhain GmbH (Traunreuth, Germany) with a resolution of 1 µm and at a contact pressure of 0.02 N/mm^2, distributed over the entire surface of the specimen. The PEG-based primer was applied in its delivered form, i.e., as a 15%-solution. The PS20-based primer was applied after dilution with deionized water to a 10%-solution, as defined in its TDS. The HMR primer's B-stage was used 3 h after adding the second portion of formaldehyde with a solid content of approx. 5% (w/w). For the application to the wood, groups of $n = 30$ specimens were immersed for 10 s into one of the three primers. A reference group was immersed into a solution of sodium hydroxide (NaOH) with a pH-value of 9, identical to the pH of the HMR primer. Subsequently, before the mass and thickness were measured, all specimens were reconditioned until they reached a constant mass. After the reconditioning of the swelling experiment, the same specimens were used for the leach-out experiment, where each specimen was immersed in 20 mL of deionized water for 72 h, with one change of water after the first day. Finally, the mass and thickness were measured again after reconditioning the samples to a constant mass. To calculate the relative change in mass $\Delta m/m_w$ and thickness $\Delta t/t_w$ due to the primer treatment as well as the leach-out procedure, m_w and t_w were used as reference values, where Δm and Δt were the change in mass and thickness, respectively.

Sorption experiments

For each wood species, the specimens were sampled from a single wood piece of approx. $4 \times 2 \times 2$ cm^3 (t×r×l). Slices with the same year rings, a radial longitudinal surface, and a thickness of approx. 200 µm were obtained using a sledge microtome. From these slices, circular specimens of 11 mm diameter were obtained using a sharp puncher. The PS20- and PEG-based primer were applied by spraying, according to their TDS and application guides, while the HMR primer was applied by brushing as suggested as the preferred method in previous publications. The amounts of primer applied to the specimens ($n = 5$) of each wood species are summarized in Table 1. For all three primers, the actual amount of active material applied to the specimens and the ratio of wood-to-primer can be found in Table SI-1.

In addition to the sorption measurements with wood, sorption measurements were also conducted with the primer components: 10 ± 0.3 mg of dried HMR

Table 1 The quantities of primer applied to the different wood species in g/m^2

	Beech	Birch	Larch	Douglas fir
HMR (B-stage)	150	150	150	150
PS20-based (10%-solution)	20	20*	10**	10
PEG-based (15%-solution)	20*	–	10	–

The HMR's B-stage was applied to all wood species with a brush. The PS20- and PEG-based primers were applied by spraying

*No application guide existed. 20 g/m^2 was selected based on the suggested amount for beech with PS20

**No application guide existed. 10 g/m^2 was selected as for the other conifer species (larch)

primer (brittle flakes of approx. 200 µm thickness), as well as 10 ± 0.3 mg of liquid PS20 concentrate and PEG, obtained from the ready-to-use mixture after air drying.

Dynamic Vapor Sorption (DVS) experiments were performed on a DVS Advantage ET equipment from Surface Measurement Systems Ltd. (London, UK). Wood specimens were placed onto the measuring pan exposing the upper and lower surface to dry the sample in situ for 6 h at 80 °C and 0% RH (nitrogen atmosphere, $N_2 \geq 99.999\%$). Directly following the drying, the temperature was reduced and kept constant for the measurement at 23 ± 0.1 °C. During the entire measurement, the specimen's mass was recorded every minute until reaching the target stop criterion of $dm/dt = 0.002\%$/min. Then, the set RH value was increased by 10%-points until the set value of 100% RH was reached, note, that the actually achieved maximum RH was ~ 96%. Subsequently, the set RH value was reduced in steps of 10%-points until 0% RH.

The experimental results for each RH-step were fitted to a double-stretched exponential (DSE) function (Eq. 1) to obtain the equilibrium moisture content (EMC) with moderately long measurement times. In Eq. (1), m/m_0 is the ratio of the specimen's mass to its respective initial mass. At the start of the measurement ($t = 0$) the ratio of m/m_0 is 1, which increases with the moisture uptake to a value > 1. The mass ratio after infinite time is described by m_{eq}/m_0. In Eq. (1), t describes the time and t_0 is the starting point of the fitted RH-step. Further, A_1 and A_2, τ_1 and τ_2, and β_1 and β_2 are the amplitude, the lifetime and the stretched exponential factor, respectively. For more details on this method, we refer to Sanchez-Ferrer et al. (2023).

$$\frac{m}{m_0} = \frac{m_{eq}}{m_0} + A_1 e^{-\left(\frac{t-t_0}{\tau_1}\right)^{\beta_1}} + A_2 e^{-\left(\frac{t-t_0}{\tau_2}\right)^{\beta_2}} \quad (1)$$

To compare the kinetics of sorption between the RH steps, the global time constant (τ) was calculated from τ_1 and τ_2 of the fitted function (Eq. 1). Therefore, an approach of minimization of the weighted sum of squares was used, which is described in detail in Sanchez-Ferrer et al. (2023).

To obtain a sorption isotherm, the EMC-values obtained with the DSE function of each RH-step were fitted to the modified GAB-model (Anderson 1946;

De Boer 1968; Guggenheim 1966) by Viollaz et al. (1999) (Eq. 2). This equation consists of the water activity (a_w = RH/100) and the fitting parameters M_0, C, K and N. Prior to the fitting, the previously obtained m_{eq}/m_0 of each measured RH-step were transferred to $\Delta m/m_0$ by the relation $\Delta m = m_{eq} - m_0$.

$$\frac{\Delta m}{m_0} = \frac{M_0 CKa_w}{\left(1 - Ka_w\right)\left(1 + (C-1)Ka_w\right)} + \frac{M_0 CKN(a_w)^2}{\left(1 - Ka_w\right)\left(1 - a_w\right)} \tag{2}$$

Based on the fitted isotherms, the moisture content from accessible sorption site occupancy (SSO) EMC^0_{SSO}, which describes the maximum amount of bound water, was calculated. For the calculation a modified version of the SSO model by Willems (2014, 2015) was applied, which is described in detail in Sanchez-Ferrer et al. (2023). First, the exponent n is determined as the minimum slope of log EMC as a function of log a_w, which occurs at $a_w^* \approx 0.25$ in wood isotherms. The function of bound water content EMC_{SSO} (Eq. 3) was then fitted to the sorption isotherm (modified GAB-model) in the lower hygroscopic range of $0 < RH < a_w^*$ to determine EMC^0_{SSO}. The non-bound water was obtained by subtracting the EMC^0_{SSO} from the sorption isotherm (modified GAB-model).

$$EMC_{SSO} = EMC^0_{SSO} a_w^n. \tag{3}$$

Permeability and diffusivity experiments

From a single board of beech, three strips of $15 \times 3 \times 300$ mm^3 (r×t×l) were cut out next to each other. Each strip contained the same year rings and had a radial longitudinal surface. The thickness of the strips was reduced to 1.0 mm using a precision planer, and subsequently, the stripes were cut into 15 mm long sections. A 13 mm diameter puncher was used for obtaining a circular specimen. The specimens were then immersed in water for 1 h and reacclimatized to constant mass at 20 ± 1 °C/65 ± 3% RH three times in order to remove stresses, with around one week between each iteration. For the primer treatment, groups of $n = 8$ specimens were submerged for 30 s in the HMR primer's B-stage (3 h after the second portion of formaldehyde was added), the PS20-based primer or the delivered solution of the PEG-based primer. After carefully removing the excess water with a paper towel, the specimens were reconditioned to constant mass at 20 ± 1 °C/65 ± 3% RH, followed by measurements of the mass and thickness with the previously described precision balance and length gage.

To determine the permeability and diffusivity of the prepared specimen, dynamic vapor transport (DVT) measurements were carried out with the DVS equipment described for the sorption experiments and customized three-part specimen holders (Fig. SI-1), as described in Sanchez-Ferrer et al. (2023). A preconditioned specimen was placed between the upper and middle part of the sample holder, forcing further moisture movement through the two radial longitudinal faces of the specimen. The specimen and an aluminum dummy in an identical specimen holder were placed on each suspension of the DVS' beam balance. After an acclimatization phase at

23 °C and 65% RH for 8 h, the bottom parts of the holders with the water basin were quickly attached to the middle parts, and the 12 h lasting experiment started. The water inside the cups led to a constant RH of close to 100%, while the outer side of the specimen was exposed to 65% RH.

At the beginning of the experiment, the measured mass remained constant, which gradually changed into a linear decrease after some minutes. At the beginning of the experiment, the moisture introduced from the specimen's surface, which faces the increased RH, spreads in an exponential process within the wood, driven by diffusion. After some minutes, this introduced moisture reaches the other surface of the specimen and exits the wood to create an equilibrium with the 65% RH air at the interface. After the diffusion process decays, the linear permeability becomes predominant, which is the constant transport of moisture through the wood. To separate the diffusivity and permeability, the experimental data were fitted with a linear-exponential function (Eq. 4), as explained in more detail by Sanchez-Ferrer et al. (2023). In Eq. (4) m/m_0 describes the ratio of the specimen's mass to the initial mass at the start of the experiment. Note that m consists of m_0 plus the change of mass during the measurement (Δm). Therefore, this leads m/m_0 to be normalized to $m/m_0 = 1$ at the start of the measurement ($t = 0$). The parameters M_W, τ_r, and β are the moisture capacity, the lifetime, and the stretched exponential parameter of the diffusivity process. Further, $\dot{m}$ describes the mass flow rate of the permeability process. By knowing the specimen's thickness (l), area (A), and volume (V), as well as the difference in partial vapor pressure (Δp) adjacent to the opposing sample surfaces, the apparent permeability coefficient (P) and the apparent diffusion coefficient (D) were calculated with Eqs. (5) and (6). Both, Eqs. (5) and (6) offer a sufficient calculation of P and D to observe the influence of the three primers on the wood. However, the vapor diffusion resistance of the still air inside the measurement cup and the boundary layer resistance on the exterior side of the cup are not considered, therefore, the results of P and D shall be taken as apparent and just used for comparative purposes.

$$\frac{m}{m_0} = 1 + M_W \left(e^{-\left(\frac{(t-t_0)}{\tau_r}\right)^{\beta}} - 1 \right) + \frac{\dot{m}}{m_0}\left(t - t_0\right) \tag{4}$$

$$D = \frac{l^2 \dot{m}}{6 m_0 M_w} \tag{5}$$

$$P = \frac{l\dot{m}}{A\Delta p}. \tag{6}$$

Tensile shear strength experiments

Tensile shear strength (TSS) experiments were conducted following the procedures of EN 302-1 (2013) with wood from beech, birch, larch, and Douglas fir. In addition to the

specimen preparation described in the standard, the primers were applied as listed in Table 1.

After the application, the primed boards were given a drying time of 25 ± 5 min for the PS20- and PEG-based primers, and approx. 12 h for the HMR primer before applying the adhesive. The four wood species mentioned above were bonded with the commercially available 1c-PUR adhesive LOCTITE® HB S309 PURBOND (Henkel & Cie. AG 2015d). 175 ± 5 g/m^2 of the adhesive was applied to one board, and the second board was placed on it immediately after. After 10 min closed assembly time, the 90 min press cycle was started. For the deciduous species—beech and birch—the pressure of the press was set to 0.8 N/mm^2 and for the two conifer species—larch and Douglas fir—to 0.6 N/mm^2. The selected values are 0.2 N/mm^2 below the suggested pressure in the adhesive's TDS, but it was found in accordance with the adhesive's supplier that this way, an excessive squeeze out from the bond line is prevented in the used laboratory setup.

From each produced assembly, 10 specimens were obtained, of which always half of them were tested following procedure A1 (7 d conditioning and tested in dry conditions: 20 °C/65% RH), and the other half following procedure A4 (7 days conditioning at 20 °C/65% RH, 6 h in boiling water, 2 h in water at 20 °C, and tested in wet conditions). After measuring the TSS in a universal testing machine with wedge screw specimen holders (ZwickRoell GmbH & Co.KG, Ulm, Germany) at a constant displacement rate of 1 mm/min, the wood failure percentage (WFP) was assessed following the procedures of EN 302-1 (2013). In order to obtain a reference shear strength value for the tested wood species, solid wood specimens in the shape of the TSS specimens were produced from identical assortments as the bonded wood specimens, exposed following procedures A1 and A4, and tested as described above.

Bond line thickness and adhesive void penetration measurements

On the end grain surface (radial tangential surface) of the A1 TSS specimen, the bond line thickness (BLT) and maximum adhesive void penetration (MAP) were determined. Therefore, both end-grain surfaces of the specimen were sanded with up to 800 grit sandpaper and cleaned with compressed air. With a reflected light microscope equipped with a 3.3-megapixel Axiocam ICc3 microscopy camera (Carl Zeiss AG, Jena, Germany) and an imaging resolution of 0.6 µm/pixel, five images of each end grain surface—each covering 1.4 mm of the bond line—were taken at equidistant positions along the bond line (2.0 mm grid). To assess the BLT and MAP, the imaging software '*Leica Application Suite V4.1*' was used. To avoid observer bias, the BLT was always measured at the same horizontal position of each image. To obtain the MAP, in each image, the distance from the furthest adhesive deposit to the closest location of the bond line was measured (Fig. SI-2).

Results and discussion

Swelling and leach-out

The question arose if only the primer's water or additionally the active substances in the primers cause swelling of the wood and if those changes are reversible when reintroducing water. To be close to the actual industrial application, each primer was used in the concentration of the active substance as suggested by the manufacturer or literature. Further, since in the bonding application only a thin layer of wood is affected by the primer, a specimen thickness of 300 µm was chosen. Prior to the actual swelling experiment, the specimens were relaxed by water immersion. While the specimens' mass remained virtually unchanged, they gained on average 8.9% thickness. This shows that the water inside all three primers causes—without the active chemicals yet being involved—changes to the wood. Namely, previously compressed wood cells, i.e., from the mechanical surface preparation, are (partly) restored. This could allow easier flow and void penetration of adhesives, as well as the relaxation of the previously induced stresses in this area. Such a pretreatment of the wood is already known in industrial applications. There, water is occasionally sprayed onto the wood prior to the 1C-PUR application to ensure a sufficient amount of water for the adhesive to react with (Kägi et al. 2006). A positive effect of water spraying before bonding beech wood with 1c-PUR was observed by Kläusler et al. (2014) in dry stage testing (A1), however, in the wet stage (A4) no positive effect was seen.

On the relaxed specimens, the relative change in mass ($\Delta m/m_w$) and thickness ($\Delta t/t_w$) caused by the application of the primers, as well as after a leach-out procedure, were measured. The data are summarized in Fig. 1a and b, respectively.

As a reference measurement, one set of specimens was treated with water at a pH-value of 9, to ensure the HMR's effects are not the result of its basic nature. After the application of the alkaline water, an increase of $\Delta m/m_w$ by 0.5% was observed,

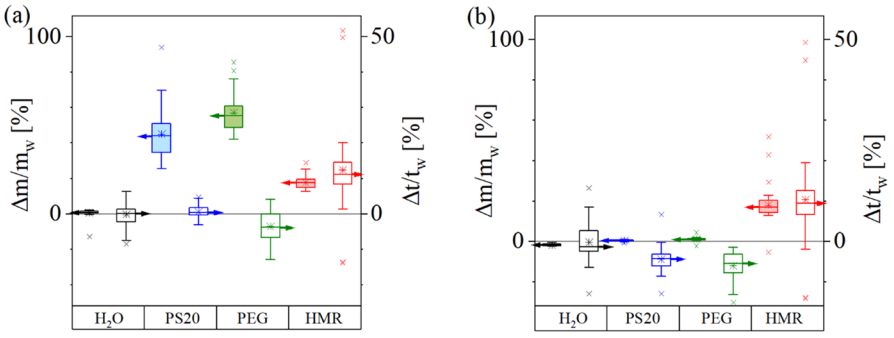

Fig. 1 Relative mass change ($\Delta m/m_w$; filled boxes) and relative change in thickness ($\Delta t/t_w$; empty boxes) of beech disks (Ø11 mm × 0.3 mm) **a** after priming and reconditioning at 20 °C and 65% RH, and **b** after the leach-out procedure by immersing the specimen for 72 h in water and reconditioning at 20 °C and 65% RH ($n = 30$). *Note* Box = 25–75 percentile, line = median, star = average, whiskers = 1.5 IQR, x = outlier

while the average $\Delta t/t_w$ virtually remained unchanged. The slight increase in $\Delta m/m_w$ could be explained by the deposition of NaOH. After the leaching procedure, $\Delta m/m_w$ was reduced to − 0.8%, assumedly from some hemicelluloses/extractives that were diluted and washed out with the alkaline water. A hydrolysis of wood polymers is not assumed at the given room temperature condition. As before, the average $\Delta t/t_w$ remained virtually unchanged, however, the median reduced to − 0.8%. As a reference measurement for the PS20 and PEG, the previously described relaxation process with water at a pH value of 7 can be taken, where no changes in $\Delta m/m_w$ and $\Delta t/t_w$ were observed.

The treatment with the PS20-based primer increased the relative mass $\Delta m/m_w$ by 45%, accompanied by an increase in the relative thickness $\Delta t/t_w$ of 0.5%, indicating a mass uptake with virtually no visible swelling of the wood cell wall structure. It could be assumed that most of the PS20 remained in the lumina of the cells. The infiltration into the cell wall results from a diffusion process, driven by the difference in the chemical potential, which could be eased by a pre-swelling of the cell wall by the low molar mass water molecules (18 g/mol). It was expected beforehand that with its molar mass of 1228 g/mol, the PS20 would infiltrate and swell the cell wall, as shown previously by Tarkow et al. (1966) for the chemically closely related PEG up to a molar mass of 3000 g/mol. This assumption remains valid, even though it is known that the PS20 in the primer is above its critical micelle concentration of 0.06 g/L (Helenius et al. 1979). These micelles consist of approx. 70 molecules of PS20 with a diameter of 7–9 nm (Basheva et al. 2007). Thus, such micelles appear too big to infiltrate into the structure of the cell wall. However, as the water of the primer evaporates or diffuses the micelles invariably come in contact with the cell walls and collapse, enabling individual PS20 molecules to diffuse into the cell wall polymers' amorphous domains but with reduced efficiency due to a lack of solvent carrier molecules and, due to that, high viscosity. Therefore, despite the presence of micelles, the here observed merely marginal increase in the specimens' thickness is still unexpectedly low. Attempting to interpret the observed behavior, it is unfortunate that no previous reports on the swelling of wood by PS20 were found in the literature. Therefore, a theoretical consideration was undertaken. The most obvious explanation is that only a small fraction of the PS20 infiltrates and swells the cell wall, meaning that the small $\Delta t/t_w$ measured, represents the actual swelling. However, it is also possible that two or more countervailing mechanisms occur in parallel. This would be the case when the PS20 infiltrates and swells the cell walls, where it acts as a plasticizer in the wood polymers' amorphous regions and, therefore, allows easier compression during the tactile thickness measurement of the thin specimens. This assumption is supported by the results of Bockel et al. (2020), who observed a reduction of the modulus of elasticity and hardness of PS20-primed beech wood by nanoindentation experiments. In addition, a follow-up experiment with thicker specimens is presented in the SI, which further supports the assumption of compression of the thin specimens during the tactile thickness measurement. After the leach-out procedure of the thin, PS20-primed specimens (Fig. 1b), nearly the original mass was obtained again, though, an increase of $\Delta m/m_w$ of 0.9% remained. It was anticipated beforehand that the PS20 would be washed out, due to the PS20's inability to form covalent bonds with the wood's polymers. The remaining, additional

mass could be explained by non-covalent interactions, e.g., hydrogen bonding, of the PS20 molecules with biopolymers inside the cell wall. Unexpectedly, instead of returning to the initial thickness, the $\Delta t/t_w$ was 4.5% below the initial value, reducing even further than with the primer. An explanation by removal of water-soluble hemicelluloses appears unlikely since no loss in mass was observed, as well as the fact that even with the alkaline reference measurement, the reduction in thickness was less than with the PS20. Also, it appears implausible that the PS20 degraded the wood's structure, which would lead to a collapse of the wood cells. It appears most reasonable that while the PS20 was removed from the lumina and assumably partly from the cell wall, the remaining PS20 in the cell wall still acted as a plasticizer. In addition, since the lumina were then filled with air instead of the liquid PS20, less force for the displacement of the lumen-filling fluid was needed, and, therefore, less resistance to compression occurred during the tactile thickness measurement.

The treatment with the PEG-based primer showed an increase in the $\Delta m/m_w$ by 57%, and the measured average $\Delta t/t_w$ decreased by 3.5%. This result looks contradicting at first. However, as already described for the PS20 primer, PEG may simultaneously cause multiple modifications of the primed wood. With the water as a carrier medium, the relatively small, linear PEG molecules (mw = 600 g/mol) can infiltrate the amorphous domains of the cell walls. After the wood dries and a new EMC is established, PEG molecules would remain in the cell wall, where they could act as plasticizers for the amorphous biopolymers. For PEG, a plasticizing effect is already known when added to synthetic polymers, e.g., poly(lactic acid) (Li et al. 2018; Pivsa-Art et al. 2016), which makes a plasticization effect with bio-based polymers also appear reasonable. As already described for the PS20, plasticization would ease compression during the tactile thickness measurement and thereby countervail an increase of thickness by the cell wall swelling. In Fig. 1b, it can be seen that during the leach-out experiment, most of the PEG is washed out, with a remaining $\Delta m/m_w$ of 0.4%, while the average thickness $\Delta t/t_w$ reduced further to 6.1% below the initial value. Analog to the PS20, it is assumed that the PEG forms non-covalent interactions with the wood biopolymers, which keeps small fractions of the PEG inside the cell wall, leading to the remaining increase of $\Delta m/m_w$. The assumption that PEG plasticizes the wood is supported by the results of Stamm (1956, 1959), who used 25% solutions of PEG of different molar masses in attempting to increase the dimensional stability and durability of Sitka spruce. Together with an increase in dimensional stability by the PEG treatment, Stamm (1956, 1959) also described a reduction of the modulus of elasticity, as well as a small swelling of the wood. Also, Schneider (1969, 1970, 1977) observed a swelling by priming spruce and beech wood with PEG of different molar mass, as well as a reduction in bending- and compression strength. Also with PEG, own measurements are presented in the SI, which support the assumption of plasticization.

The priming of the thin specimens with the HMR B-stage (3h) resulted in an increased $\Delta m/m_w$ of 18.1% and $\Delta t/t_w$ of 12.4%. After the leach-out procedure, the average $\Delta m/m_w$ and $\Delta t/t_w$ remained practically unchanged. The increased thickness after priming the specimens with the HMR indicates an obvious infiltration of primer substances into the cell wall. In addition, the specimens changed color to a darker brown. After the leaching treatment, $\Delta m/m_w$, $\Delta t/t_w$ and the color remained

unchanged, which indicates that part of the HMR ingredients chemically reacts with the wood biopolymers, establishing covalent bonds, as previously described by Yelle et al. (2016) for the chemically closely related PF adhesive. This is reasonable due to the reactive nature of the HMR. Concerning a plasticization effect by the HMR treatment, as described for the other two primers, the unchanged $\Delta m/m_w$ and $\Delta t/t_w$ do not give a base for or against such an assumption. Based on the existing literature about the HMR primer, no clear statement on its effect on the mechanical properties of the primed wood can be given, i.e., the results of Son et al. (2005) indicated a softening of the wood by the HMR treatment, whereas the results of Sun et al. (2005) indicated a stiffening.

Another mechanism that can be considered for all three primers is that they reduce further swelling of the primed wood. According to Frihart et al. (2023), a pre-swelling by deposited chemicals makes it less likely for the cell walls to further absorb water and swell hygroscopically. The observed leach-out of the PS20- and PEG-based primer is not considered to contradict this assumption. In the leach-out experiment, the thin specimens of primed wood were exposed to a high quantity of liquid water (~ 15 mg to ~ 40 g) combined with a short distance to enter and exit the specimen (~ 150 µm), and a long duration (3 days). In EWP as well as in standardized testing, e.g., delamination resistance, those extreme conditions do not apply.

To summarize, our results indicate that a fraction of the three primers' active substances penetrate the wood's cell wall and cause a swelling that exceeds the swelling of just the water in the primers' formulation. The PS20- and PEG-based primers are removable from the wood by leaching, which confirms that no covalent bonds are formed with the wood's biopolymers. The results suggest that the PS20 and PEG in the cell walls might act as plasticizers, which could ease the deformation of the affected wood. Since the HMR primer cannot be leached out again, this indicates covalent bonding with the wood's biopolymers. Unlike the other two primers, the data do not allow conclusions about whether the HMR primer influences the mechanical properties of the primed wood.

Sorption

It was expected that the application of a primer would modify the water uptake and sorption kinetics of the primed wood, thus, influencing the formation of moisture-induced stresses in the bond line region. Dynamic vapor sorption experiments at different RH values were performed, which determined the EMC and the water sorption kinetics of unprimed wood, primed wood, and the pure active substance of the primers.

The sorption isotherms of unprimed and primed beech wood are shown in Fig. 2a, while the isotherms of unprimed and primed birch, larch, and Douglas fir are found in Fig. SI-3. All isotherms have an S-shape with a hysteresis loop (Type IV), as is typical for porous materials, including wood (Sing et al. 1985). Compared to the unprimed wood, the HMR primer caused for all wood species a small increase in the EMC during both the adsorption and desorption processes below 90% RH, while above 90% RH being slightly below. With the

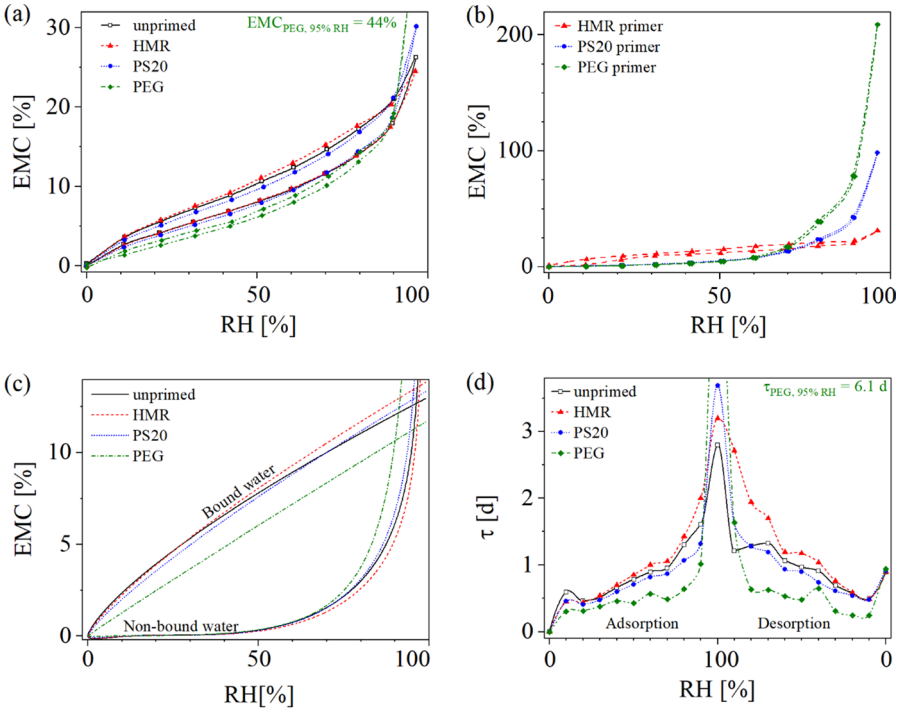

Fig. 2 **a** Moisture sorption isotherms of unprimed and primed beech wood ($n=5$). **b** Moisture sorption isotherms of primers' pure active substances ($n=5$). **c** Bound and non-bound water distribution following the SSO model of unprimed and primed beech wood. **d** The time constant (τ) of the unprimed and primed beech wood ($n=5$)

PS20- and PEG-based primer, the EMC reduced in adsorption and desorption below 90% RH, while above this value the EMC surpassed the unprimed wood. These observed effects of the PEG-based primer on beech wood are in line with the findings of Schneider (1969), whose treatment of spruce with PEG 400 and PEG 1000 (Fig. SI-4) resulted in comparable changes in the sorption as observed here.

In order to better understand the observed changes in the wood's sorption isotherms, the same measurements were performed with the pure active substance of each primer (Figs. 2b, SI-5a). The isotherm of the solid, cured HMR primer had an S-shape with a hysteresis loop (Type IV, porous material). Over the entire RH range, the EMC of the pure HMR primer was approximately 4–6%-points above the EMC of the unprimed wood. While in the literature, no sorption isotherm was found for HMR to compare with, Wimmer et al. (2013) reported for the chemically related PRF-adhesive also a type IV isotherm, but approximately 5%-points below the HMR's sorption isotherm in this study (Fig. SI-5c). Due to the high water content of the HMR primer during curing, it appears reasonable that HMR forms a less dense network with more unreacted sorption sites compared to the PRF adhesive.

The isotherms of the liquid PS20- and PEG-based primers were convex without a hysteresis loop (Type III, non-porous materials). Below 60% RH, both substances behaved nearly identically with EMC values 0.5–6%-points below the unprimed wood. Above 60% RH, the EMC of both substances rose rapidly and exceeded the EMC of wood. This rise resulted from the high compatibility of both substances with water, as further indicated by the final EMC-value near the air's saturation with water vapor (~96% RH) of around 100% and 200% for PS20 and PEG, respectively. When comparing the obtained sorption isotherm of the pure PS20 from this study with a measurement of Asmus et al. (2016), the results are *quasi*-congruent (Fig. SI-5c). The obtained sorption isotherm of the PEG shows high similarities with the PEG 400 and PEG 1000 isotherms shown by Schneider (1969), as well as the PEG 1450 by Baird et al. (2010) (Fig. SI-5d). However, the sorption isotherm of the primer's PEG is in between the one of the PEG 400 and the PEG 1000, which is reasonable for a PEG with a molar mass of 600 g/mol.

When combining the previously presented EMC of the primed wood and the pure primers, it can be seen that the EMC of the primed wood shifts toward the primers' EMC. However, this similarity does not explain the clear difference between the PS20- and PEG-based primer, which leads to a further analysis of the available sorption sites.

On the measured sorption isotherms, the modified GAB model was used for interpolation purposes, while the SSO model was used to analyze the quantities of bound and non-bound water and, therefore, gain information on the available sorption sites of the unprimed and primed wood. In Fig. 2c, the deconvolution of the adsorption isotherms into bound and non-bound water profiles of beech wood is presented. For birch, larch, and Douglas fir, the corresponding results can be found in Fig. SI-6.

In the sorption isotherm of HMR-primed beech, the SSO model reveals an increase of bound water. With the HMR-primed birch, larch, and Douglas fir, similar results were obtained. When looking at the literature value for available hydroxyl groups of beech wood of 7.5 mmol/g (Bockel et al. 2020) and 7.9 mmol/g (Fredriksson et al. 2023) and 15.6 mmol/g of HMR, the observed increase in the bound water becomes reasonable. Therefore, it is concluded that with HMR priming, the number of available sorption sites inside the wood increases. Even though the HMR occupies some sorption sites of the wood during its curing, the new sorption sites from the cured HMR do not just compensate for those but even exceed the number of sorption sites occupied.

The treatment with the PS20-based primer of beech, birch, and Douglas fir caused a slight decrease in the bound water fraction, while for larch wood, the decrease in the bound water was more pronounced. The PS20 has, with 2.4 mmol/g, a lower number of sorption sites and, therefore, less available hydroxyl groups, compared to the wood which is in the region of 6–11 mmol/g (Fredriksson et al. 2023). Thus, the resulting number of sorption sites in the different wood species after applying PS20 resulted in a lower fraction of bound water molecules. Bockel et al. (2020) observed a more intense reduction of accessible OH-groups by deuterium exchange after PS20 priming on beech wood from 7.5 mmol/g to 5.5 mmol/g. The more intense reduction observed by Bockel et al. (2020) compared to the results obtained here, speculatively results from the use of different methods, i.e., one sorption step with

deuterium oxide ('heavy water') vs. a sorption isotherm from water processed with a model.

The treatment with the PEG-based primer on beech and larch caused a clear decrease in the bound water. The available sorption sites of PEG 400, PEG 600, and PEG 1000 are, with 5.0 mmol/g, 3.3 mmol/g, and 2.0 mmol/g, respectively, clearly below the values for wood. This supports the observed reduction of the bound water by the PEG priming. In parallel, it raises the question of why it reduces the EMC and bound water much stronger than the PS20 with 2.4 mmol/g while the ratio of wood to primer for both treatments is *quasi*-identical. The difference in the molar mass between PS20 and PEG was discarded to be the source of the phenomena since Schneider (1969) obtained with PEG 400, PEG 1000, and PEG 4000 (Fig. SI-4) always similar reductions of the wood's EMC, only differing at which RH the quick rise of the EMC begins. However, major differences between PEG and PS20 can be found in the hydrophilicity and structure of the molecules. The hydrophilic PEG molecules are more compatible with the hydrophilic components of the wood compared to the amphiphilic PS20. It appears reasonable that the OH-groups and ether groups form non-covalent interactions that prevent moisture from reaching the OH-groups of the wood. This allows the PEG to remain in close proximity to the hydrophilic wood compounds, blocking water molecules from having access to the wood's otherwise available sorption sites. All that is further supported by slower curing of the adhesive on the primed wood, which is reflected in the longer, required pressing time in the primer TDS. With the PS20, less dense packing can be expected.

To gain further information on the kinetics of the processes during sorption, the global time constant (τ) was retrieved for each RH step. In Fig. 2d, the time constant profiles as a function of the RH for the unprimed and primed beech wood are shown. The time constant profiles for birch, larch, and Douglas fir are shown in Fig. SI-7 and for the pure primers in Fig. SI-5b.

For the HMR-primed wood samples, slower water diffusion kinetics – therefore, higher time constant values—were observed than those from unprimed wood in all wood species. This effect clearly comes from the HMR's structure, for which the time constant is very high (Fig. SI-5b), indicating that the cured primer works as a solid barrier with a porous structure where water molecules are trapped and diffuse very slowly.

The PS20- and PEG-primed wood samples show faster water diffusion kinetics—and lower time constant values—than the unprimed wood, below 90% RH. The PS20- and PEG-based primers enhance the diffusion of water molecules through the wood structure due to their high compatibility/solubility with water and due to their liquid nature that allows for a fast exchange/mobility of the water molecules. This also becomes evident in the time constant of pure PS20 and PEG, which, below 60% RH, are below the values from wood (Fig. SI-5b). However, above 90% RH, when approaching the fiber saturation region, the time constant values increase above the unprimed wood (Fig. SI-7), and due to the high quantity of water, the pure primers are capable of retaining.

To summarize, the three primers have different effects on the wood's sorption behavior. The HMR primer slightly increases the EMC of the primed wood by offering additional sorption sites. Moreover, the cured and solid HMR components slow

down the kinetics of the water uptake because they act as a physical barrier, which probably leads to a slower build-up of moisture-induced stresses. The PS20 primer slightly decreases the EMC of the primed wood by impeding the water's access to the wood's available OH groups. In parallel, it accelerates the kinetics of the water uptake due to its liquid nature. With the liquid and fully hydrophilic PEG primer, the reduced EMC and the increased kinetics are more pronounced compared to those of the PS20 primer, which is amphiphilic. The PEG molecule stays in close proximity to the hydrophilic components of the wood, preventing water from reaching the wood's OH groups. Due to the shown pronounced effects on the sorption, these changes on the wood are supposed to be relevant to the primers' positive effect on the bond performance.

Permeability and diffusivity

It was expected beforehand that the presence of a primer affects the kinetics of the moisture uptake and moisture transport capacity and, thereby, the build-up of stresses in the interphase zone. The apparent diffusivity coefficient (D) was measured by removing a wood disk from its equilibrium state at 65% RH and exposing one surface to 100% RH. Based on the forced mass flow through the specimen, the apparent permeability coefficient (P) was also measured. The applied method is well suitable to compare the impact of the primers, nevertheless, due to its apparent nature, a deviation to the specific P and D values can be expected.

The apparent permeability and diffusivity coefficients of primed and unprimed beech wood are illustrated in Fig. 3a and b, respectively. The average permeability coefficient value is $5.9 \cdot 10^{-10}$ mol/(m s Pa), $5.5 \cdot 10^{-10}$ mol/(m s Pa), $5.8 \cdot 10^{-10}$ mol/(m s Pa), and $6.1 \cdot 10^{-10}$ mol/(m s Pa), for unprimed beech wood, and primed with PS20, PEG, and HMR, respectively. The average diffusion coefficient value is $5.9 \cdot 10^{-11}$ m^2/s, $4.7 \cdot 10^{-11}$ m^2/s, $4.0 \cdot 10^{-11}$ m^2/s, and $8.3 \cdot 10^{-11}$ m^2/s, for unprimed beech wood, and primed with PS20, PEG, and HMR, respectively.

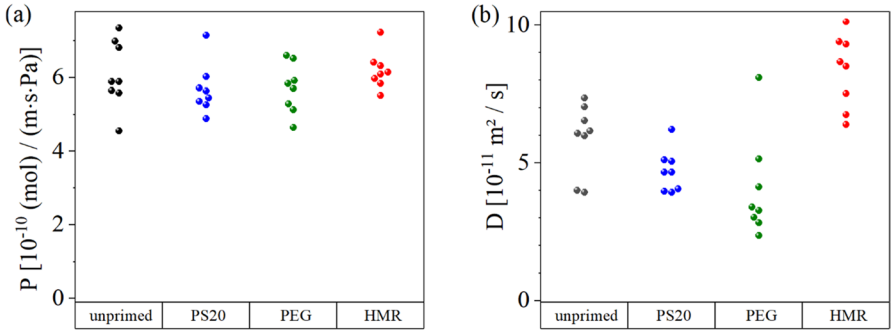

Fig. 3 **a** Apparent permeability coefficient (P), and **b** apparent diffusion coefficient (D), measured on thin disks of unprimed, and primed beech wood ($n = 8$), with 65% RH and 100% RH on each side of the wood sample

The results for the permeability coefficient, as well as for the diffusion coefficient, spread over a rather wide range. This is believed to result from the fluctuations in the properties of the wood, even though it was taken great care to use specimens with as few variations as possible.

For the permeability values, no significant differences between the unprimed wood and the wood primed with the three different primers can be noticed. This means that the moisture flow of unprimed and primed wood is rather the same.

The diffusivity values with the PS20 and PEG treatment are notably lower compared to the unprimed wood. This can be explained by the hydrophilic branches of the amphiphilic PS20 and the entirely hydrophilic PEG molecules. With the HMR primer, the diffusivity rises above the unprimed wood.

Permeability, diffusion and sorption are related properties ($S = P/D$). Due to the *de facto* constant permeability, a reduced diffusion must be accompanied by increased sorption and *vice versa*. As shown in the upper region of the sorption isotherms (65–100% RH), the previously described relationship is confirmed (Fig. SI-8 and Table SI-2). By dividing the permeability by the diffusion, the obtained sorption values are 10.0 mol/(m^3 Pa), 11.6 mol/(m^3 Pa), 14.3 mol/(m^3 Pa), and 7.3 mol/(m^3 Pa) for beech wood unprimed and primed with PS20, PEG, and HMR, respectively. Based on the sorption isotherms, also the sorption values were calculated by taking into account the values from 65 to 98% RH, as described in more detail in Fig. SI-8 and Table SI-2. The this way obtained sorption values are 3.83 mol/(m^3 Pa), 4.10 mol/(m^3 Pa), 4.71 mol/(m^3 Pa), and 3.79 mol/(m^3 Pa) for unprimed wood and primed with PS20, PEG, and HMR, respectively. It becomes evident that the results from both approaches follow the same trend. The HMR primed wood has the lowest sorption, slightly below the unprimed wood, followed by the PS20 primed and, finally, the PEG-primed wood. The differences in the absolute sorption values are believed to result from the different methodologies of both measurements, i.e., the vapor exposure only to the radial longitudinal surfaces (DVT) vs. the exposure to all surfaces of the specimen (DVS), and the different application methods of the primers.

To summarize, the primer treatment has no significant effect on the wood's permeability. However, the water diffusion is slightly decreased after the HMR priming, while it increases with the PS20 and PEG priming, which is in line with the previously obtained sorption measurements.

Bond line thickness and adhesive void penetration

Since primers are applied prior to the adhesives onto the same surface of specimens, it was assumed that they influence the bulk flow of the adhesive into the interphase zone (void penetration) and, therefore, the bond line properties. The inspection of bonded specimens was conducted via reflected light microscopy where the bond line thickness (BLT) and the maximum adhesive void penetration (MAP) were measured in order to evaluate the effect due to the presence of the different primers.

In Fig. 4a, the BLT and MAP values of 1C-PUR bonded beech wood with and without primer treatment are shown, while the detailed results for birch, larch, and

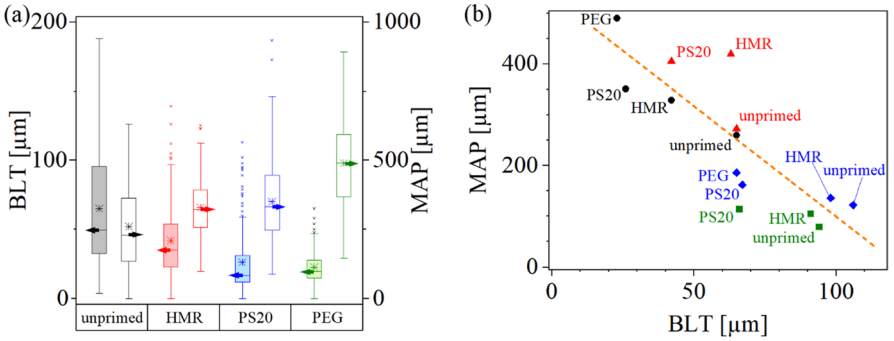

Fig. 4 **a** Bond line thickness (BLT; filled boxes) and maximum adhesive void penetration (MAP; empty boxes) of the 1c-PUR bonded beech wood specimens after TSS measurements ($n = 150$). *Note* Box = 25–75 percentile, line = median, star = average, whiskers = 1.5 IQR, x = outlier. **b** MAP as a function of the BLT for the four different wood species (black circle = beech; red triangle = birch; blue diamant = larch; green square = Douglas fir) with or without any priming. (correlation function: MAP = 535–4.4 BLT; $R^2 = 0.8$). Note: There is for each wood species an order that can be related to a retention-reducing effect of the primer (unprimed wood – HMR – PS20 – PEG) (color figure online)

Douglas fir can be found in Fig. SI-9. Unprimed beech samples show average BLT and MAP values of 65 µm and 260 µm, respectively, while HMR-primed beech samples have 42 µm and 329 µm, respectively. PS20-primed beech samples have average BLT and MAP values of 26 µm and 351 µm, respectively, and PEG-primed beech samples have values of 23 µm and 490 µm, respectively. It can be deduced for beech wood bonded with 1c-PUR that all primer treatments caused an increase in the adhesive's void penetration depth, which goes in line with a corresponding reduction of the bond line thickness. Since similar results were also observed with the other three wood species, the relation of BLT and MAP for all species and primers are compared, as shown in Fig. 4b. Based on the recommendation of the PEG-based primer's commercial distributor—to only be suitable for larch wood—it was only used on larch wood and—as a contrasting test—on beech wood, while birch and Douglas fir were omitted and therefore cannot be found in Fig. 4b.

The increase in the adhesive's void penetration has a direct impact on the thickness of the bond line, which reduces because the adhesive that penetrated into the wood's voids is no longer available for the bond line formation. Industrial users reported the need to apply more 1c-PUR adhesive to achieve the same BLT value as without primer when using PS20- and PEG-based primers, which supports our findings.

According to Kamke et al. (2007), the void penetration of the still liquid adhesive is mainly caused by hydrodynamic flow, e.g., by applying pressure during the clamping, and capillary action. Here, the liquid adhesive flows into the interconnected network of the wood cells, consisting of lumina of tracheids, vessels, fibers, and wood rays and pits. A well-known model to calculate a liquid's capillary flow is the Lucas-Washburn equation (Lucas 1918; Washburn 1921). While it gives a good basic approach, the given complexity exceeds the model's framework conditions, i.e., the adhesive's change in viscosity and surface tension due to curing, more

than a single, homogeneous liquid, and modifications of the capillary's surfaces, and therefore does not allow it to be applied here. However, with the Lucas-Washburn equation and its limitations in mind, the following considerations are made. With the liquid PS20 and PEG primers, it appears reasonable that they create a low viscose layer on the interface of the lumina to the S3 cell wall layer that reduces the retention of the adhesive during the pressing process. The cured HMR on the other hand creates a rather hydrophobic, solid layer that is more compatible with the 1c-PUR adhesive and reduces the retention. Another explanation for all three primers is the restrain of water from the wood to the not-yet-cured adhesive. This leads to a slower curing of the 1c-PUR adhesive—accompanied by a slower increase of viscosity—which gives the adhesive additional time to penetrate into lower sub-regions of the wood.

Independent of the reasons, the increased void penetration counteracts what Hunt et al. (2018) describe as an 'underpenetration'. They describe the results to be a too-small bonding surface, therefore, not enough mechanical interlocking, or the adhesive not to surpass the weak boundary layer of the wood. Hunt et al. (2018) further postulate that after reaching a sufficient level of void penetration, further void penetration does not lead to an improved bond performance, while just increasing the consumption of adhesive required to form a sufficient bond line.

To summarize, the use of primers assists the 1c-PUR adhesive to penetrate deeper into the wood, leading to increased mechanical interlocking. However, this also goes in line with a higher adhesive grammage in order to achieve the intended bond line thickness.

Tensile shear strength

In order to validate the previously reported positive impact of the primers' on the bond performance, tensile shear specimens were produced. Following two different moisture exposure and conditioning treatments, the specimens were loaded until fracture, and the tensile shear strength (TSS), as well as the wood failure percentage (WFP), were evaluated.

In Fig. 5, the results of beech wood bonded with 1c-PUR are presented, while the results for larch, birch, and Douglas fir, can be found in Fig. SI-10. In the dry stage (A1), the average TSS (WFP) was 14.4 N/mm^2 (39%), 14.9 N/mm^2 (100%), 17.3 N/mm^2 (65%), and 14.2 N/mm^2 (74%) for the unprimed, HMR, PS20, and PEG primed beech wood, respectively. All TSS results were consistently above the 10 N/mm^2 required by EN 15425 (2017) and comparable to or above the solid wood reference with 14.4 N/mm^2 (100%). In the wet stage (A4), the TSS (WFP) was 3.5 N/mm^2 (2%), 7.7 N/mm^2 (100%), 6.9 N/mm^2 (22%), and 4.8 N/mm^2 (0%) for the unprimed, HMR, PS20, and PEG primed beech wood, respectively. When comparing the results to the 9.5 N/mm^2 (100%) of the solid wood, regardless of the priming, all values are below this reference. The minimum requirement of 6 N/mm^2 for A4 in EN 15425 (2017) was met with the HMR and the PS20 primer but not with the unprimed and PEG-primed wood. In this context, it is important to note that the

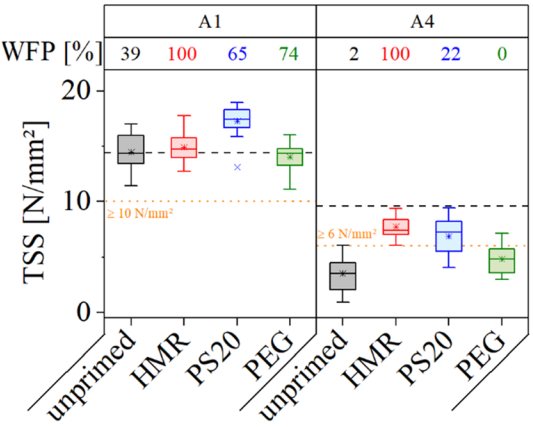

Fig. 5 Tensile shear strength (TSS) values and the wood failure percentage (WFP) of beech wood bonded with 1c-PUR adhesive for unprimed wood (gray), treated with HMR primer (red), PS20 primer (blue) and PEG primer (green). The black dashed line represents the TSS value for solid beech wood, and the orange dot line represents the minimum TSS required value in EN15425 ($n = 15$). Note: box = 25–75 percentile, line = median, star = average, whiskers = 1.5 IQR, x = outlier (color figure online)

PEG primer was not developed for beech wood but for larch, where it shows significant improvements in bond performance (Fig. SI-10).

Using the same adhesive and test method Kläusler et al. (2014) achieved similar results for unprimed and HMR-primed beech wood. The TSS (WFP) was 12.4 N/mm^2 (80%) and 13.6 N/mm^2 (85%) in A1 and 6.2 N/mm^2 (15%) and 7.0 N/mm^2 (60%) in A4, respectively. Konnerth et al. (2016) used the same adhesive and test method and obtained with the PS20 primer in A1 treatment with beech 11.7 N/mm^2 (100%) and with birch 12.5 N/mm^2 (93%), as well as 6.8 N/mm^2 (44%) and 5.7 N/mm^2 (54%) in A4, respectively. In A1 with unprimed larch wood, they obtained 8.7 N/mm^2 (100%) and in A4 2.5 N/mm^2 (2%). Showing the same tendencies, the results for the different wood species and treatments by Kläusler et al. (2014) and Konnerth et al. (2016) support the results obtained in this study (Figs. 5 and SI-10).

In summary, the use of the three primers resulted for all four tested wood species in an improvement of the tensile shear strength, compared to the unprimed wood, showing that the use of primers can increase the bond quality and performance of EWP when using 1c-PUR adhesives.

Conclusion

The motivation of the presented research was to extend the understanding of the functionality of the HMR, PS20 and PEG primer, focusing on their interactions with water and wood.

All three primer systems consist predominantly of water during their application, which leads to a swelling of the wood cell walls by the water molecules in the interphase zone. At the same time, this swelling by the water facilitates the infiltration

of the primers' active substances into the wood cell walls. Inside the cell walls, the primer's active substances also cause swelling, e.g., 18% with the HMR primer. But, unlike when caused by water, this swelling remains after the wood re-dries. This mechanism could explain the better bond performance when tested in the wet stage, e.g., delamination test or TSS after A4 water treatment. The PS20 and the PEG primer cause a plasticization effect inside the cell walls. When the primed wood gets exposed to stresses, it is assumed that the stresses are distributed away from the adhesive layer, also in the dry stage. The PS20 and PEG molecules form non-covalent bonds, i.e., hydrogen bonds, with the wood biopolymers but remain water-soluble and liquid. A distinctive feature of the HMR primer is that its solid compounds crosslink and form covalent bonds with the wood biopolymers. Consequently, the HMR primer becomes insoluble and cannot move or be removed from the cell wall, e.g., by water exposure.

The treatment with the HMR, PS20 and PEG primer influences the water sorption capacity and diffusivity of wood while its permeability remains unaffected. However, the changes in sorption and diffusivity appear rather small to play the primary role regarding the positive effects on the bond performance. The analysis of the moisture sorption isotherms, using an SSO model, shows that the EMC values are influenced by the number of sorption sites affected by the primer treatment.

All three primer systems increase the void penetration of the 1c-PUR adhesive into the wood-bond line interphase, i.e., 88% with PEG, 35% with PS20 and 26% with HMR. One possible explanation is the reduced retention of the adhesive during the pressing of the two adherents. It is suggested that the primers' active substances are deposited on the S3 surface of the conducting cells (e.g., earlywood tracheids in softwoods, vessels in hardwoods) and allow an easier flow of the adhesive into the interphase zone. In addition, the deposited primers' active substances possibly retard the adhesive's curing due to a restrain of water molecules, which are needed to react with the prepolymers. This leads to a slower rise of viscosity, which gives the adhesive more time to penetrate into deeper zones of the interphase region.

From our research, it becomes obvious that even though the primers serve the same purpose—improving the bond performance in dense or extractive-rich wood species under moist conditions—their mechanisms to achieve this goal are different. However, the presented details on the primer's mode of action might help to continue our efforts to integrate the functionalities of primers directly into the adhesive systems to eliminate the need for the previous 2-step application.

Supplementary Information The online version contains supplementary material available at https://doi.org/10.1007/s00226-023-01508-z.

Acknowledgements The authors gratefully acknowledge the funding from the Bavarian State Institute of Forestry. The data used in this publication are available from the authors upon reasonable request. The authors gratefully acknowledge Roland Braun who skillfully prepared the wood samples and Frank Moosmann, who supported the laboratory work.

Author contributions All authors contributed to the study's conception and design. Material preparation, data collection, data processing, and analysis were performed by TB, ME, FTS, and ASF. The first draft of the manuscript was written by TB, and all authors commented on previous versions of the manuscript. All authors read and approved the final manuscript.

Funding Open Access funding enabled and organized by Projekt DEAL.

Declarations

Conflict of interest The reported research is financed by the Bavarian State Institute of Forestry (Germany) with Grant number X044. The authors have no relevant financial or non-financial interests to disclose.

Consent for publication This article has not been published previously and is not under consideration for publication elsewhere. Its publication is approved by all authors and by the responsible authorities where the work was carried out. If accepted, this work will not be published elsewhere including electronically in the same form, in English or in any other language, without the written consent of the copyright-holder.

References

Amen-Chen C, Gabriel J (2015) Wet adhesion durability improvement of polyurethane wood adhesives with primer. Eur J Wood Prod 73:697–700. https://doi.org/10.1007/s00107-015-0942-9

Amen-Chen C, Gabriel J (2020) Adhesive system for lignocellulosic substrates having high levels of extractives. European Patent No. 2 848 638, European Patent Office

Anderson RB (1946) Modifications of the Brunauer, Emmett and Teller equation. J Am Chem Soc 68:686–691. https://doi.org/10.1021/ja01208a049

Asmus E, Popp C, Friedmann AA, Arand K et al (2016) Water sorption isotherms of surfactants: a tool to evaluate humectancy. J Agric Food Chem 64:5310–5316. https://doi.org/10.1021/acs.jafc.6b01378

ASTM D 907 (2015) standard terminology of adhesives, ASTM International, West Conshohocken, PA (USA)

ASTM D 2559 (2004) Standard specification for adhesives for structural laminated wood products for use under exterior (wet use) exposure conditions, ASTM International, West Conshohocken, PA (USA)

Baird JA, Olayo-Valles R, Rinaldi C, Taylor LS (2010) Effect of molecular weight, temperature, and additives on the moisture sorption properties of polyethylene glycol. J Pharm Sci 99:154–168. https://doi.org/10.1002/jps.21808

Basheva ES, Kralchevsky PA, Danov KD, Ananthapadmanabhan KP et al (2007) The colloid structural forces as a tool for particle characterization and control of dispersion stability. Phys Chem Chem Phys 9:5183–5198. https://doi.org/10.1039/B705758J

Bockel S, Harling S, Grönquist P, Niemz P et al (2020) Characterization of wood-adhesive bonds in wet conditions by means of nanoindentation and tensile shear strength. Eur J Wood Prod 78:449–459. https://doi.org/10.1007/s00107-020-01520-1

Böger T, Sanchez-Ferrer A, Richter K (2022) Hydroxymethylated resorcinol (HMR) primer to improve the performance of wood-adhesive bonds—a review. Int J Adhes Adhes 113:103070. https://doi.org/10.1016/j.ijadhadh.2021.103070

Casdorff K, Kläusler O, Gabriel J, Amen C et al (2018) About the influence of a water-based priming system on the interactions between wood and one-component polyurethane adhesive studied by atomic force microscopy and confocal Raman spectroscopy imaging. Int J Adhes Adhes 80:52–59. https://doi.org/10.1016/j.ijadhadh.2017.10.001

Cheng RX, Gu JY (2010) Study of improvement of bonding properties of Larch glued laminated timber. Pigm Resin Technol 39:170–173. https://doi.org/10.1108/03699421011040802

Christiansen AW (2005) Chemical and mechanical aspects of HMR primer in relationship to wood bonding. For Prod J 55:73–78
Christiansen AW, Okkonen EA (2003) Improvements to hydroxymethylated resorcinol coupling agent for durable bonding to wood. For Prod J 53:81–84
Christiansen AW, Vick CB, Okkonen EA (2000) A Novolak-Based Hydroxymethylated Resorcinol Coupling Agent for Wood Bonding. In Wood Adhesives, edited by USDA Forest Service FPL. Forest Products Society, South Lake Tahoe, pp 245–250
Clerc G, Lehmann M, Gabriel J, Salzgeber D et al (2018) Improvement of ash (*Fraxinus Excelsior* L.) bonding quality with one-component polyurethane adhesive and hydrophilic primer for load-bearing application. Int J Adhes Adhes. https://doi.org/10.1016/j.ijadhadh.2018.06.017
CSA O112.9-10 (2014) Evaluation of adhesives for structural wood products (exterior exposure), CSA Group, Ontario (Canada)
De Boer JH (1968) The dynamical character of adsorption. Oxford Univeristy Press, Oxford
Ebnesajjad S (2011) Characteristics of Adhesive Materials. In: Ebnesajjad SC (ed) Handbook of adhesives and surface preparation, Chapter 8. William Andrew Publishing, Norwich. https://doi.org/10.1016/b978-1-4377-4461-3.10008-2
EN 302-1 (2013) Adhesives for load-bearing timber structures - Test methods - Part 1: Determination of longitudinal tensile shear strength, Beuth Verlag, Berlin
EN 15425 (2017) Adhesives - One component polyurethane (PUR) for load-bearing timber structures - Classification and performance requirements, Beuth Verlag, Berlin
Fredriksson M, Rüggeberg M, Nord-Larsen T, Beck G et al (2023) Water sorption in wood cell walls–data exploration of the influential physicochemical characteristics. Cellulose 30:1857–1871. https://doi.org/10.1007/s10570-022-04973-0
Frihart CR (2009) Adhesive groups and how they relate to the durability of bonded wood. J Adhes Sci Technol 23:601–617. https://doi.org/10.1163/156856108X379137
Frihart CR, Konnerth J, Frangi A, Gottlöber C et al (2023) Joining and Reassembling of Wood. In: Niemz P, Teischinger A, Sandberg D (eds) Springer Handbook of Wood Science and Technology, Chapter 14. Springer International Publishing, Cham. https://doi.org/10.1007/978-3-030-81315-4_14
Gardner DJ, Frazier CE, Christiansen AW (2005) Characteristics of the wood adhesion bonding mechanism using hydroxymethyl resorcinol. In: Frihart Charles R (ed) Wood Adhesives. Forest Products Society, San Diego
Guggenheim EA (1966) Application of statistical mechanics. Oxford University Press, Oxford
Helenius A, McCaslin DR, Fries E, Tanford C (1979) Properties of detergents. In: Fleischer S, Packer L (eds) Methods in Enzymology. Academic Press, Cambridge. https://doi.org/10.1016/0076-6879(79)56066-2
Henkel & Cie. AG (2015a) Application guide: Surface bonding of BEECH-wood with the primer LOCTITE PR 3105 PURBOND and LOCTITE® HB S PURBOND-adhesive [in German], Sempach Station, Switzerland: Henkel & Cie. AG
Henkel & Cie. AG (2015b) Application guide: Surface bonding of DOUGLAS FIR-wood with the primer LOCTITE PR 3105 PURBOND and LOCTITE® HB S PURBOND-adhesive [in German], Sempach Station, Switzerland: Henkel & Cie. AG
Henkel & Cie. AG (2015c) Application guide: Surface bonding of LARCH-wood with the primer LOCTITE PR 7010 PURBOND and LOCTITE® HB S PURBOND-adhesive [in German], Sempach Station, Switzerland: Henkel & Cie. AG
Henkel & Cie. AG (2015d), LOCTITE® HB S309 PURBOND. Technical Data Sheet [in German]. Sempach Station, Switzerland: Henkel & Cie. AG
Henkel & Cie. AG (2017) LOCTITE® PR 7010 PURBOND. Technical Data Sheet [in German]. Sempach Station, Switzerland: Henkel & Cie. AG
Henkel & Cie. AG (2018), LOCTITE® PR 3105 PURBOND. Technical Data Sheet [in German]. Sempach Station, Switzerland: Henkel & Cie. AG
Hunt CG, Frihart Charles R, Dunky M, Rohumaa A (2018) Understanding wood bonds-going beyond what meets the eye: a critical review. Prog Adhes Adhes. https://doi.org/10.1002/9781119625322.ch8
Kägi A, Niemz P, Mandallaz D (2006) Influence of moisture content and selected technological parameters on the adhesion of one-part polyurethane adhesives under extreme climatical conditions. Holz Roh- Werkst 64:261–268. https://doi.org/10.1007/s00107-005-0088-2

Kläusler O, Hass P, Amen C, Schlegel S et al (2014) Improvement of tensile shear strength and wood failure percentage of 1C PUR bonded wooden joints at wet stage by means of DMF priming. Eur J Wood Prod 72:343–354. https://doi.org/10.1007/s00107-014-0786-8

Kamke FA, Lee JN (2007) Adhesive penetration in wood—a review. Wood Fiber Sci 39:205–220

Konnerth J, Kluge M, Schweizer G, Miljković M et al (2016) Survey of selected adhesive bonding properties of nine European softwood and hardwood species. Eur J Wood Prod 74:809–819. https://doi.org/10.1007/s00107-016-1087-1

Lehringer C, Amen C, Gabriel J (2014) Innovations in the bonding of larch wood and alternative types of wood with 1C-PURBOND adhesives. Holzverbindungen mit Klebstoffen für die Bauanwendung. Swiss Wood Innovation Network, Weinfelden, pp 123–127

Li D, Jiang Y, Lv S, Liu X et al (2018) Preparation of plasticized poly (lactic acid) and its influence on the properties of composite materials. PLoS ONE 13:e0193520. https://doi.org/10.1371/journal.pone.0193520

Lucas R (1918) Ueber das Zeitgesetz des kapillaren Aufstiegs von Flüssigkeiten. Kolloid-Zeitschrift 23:15–22. https://doi.org/10.1007/BF01461107

Luedtke J, Amen C, Ofen A, Lehringer C (2015) 1C-PUR-bonded hardwoods for engineered wood products: influence of selected processing parameters. Eur J Wood Prod 73:167–178. https://doi.org/10.1007/s00107-014-0875-8

Okkonen EA, Vick CB (1998) Bondability of salvaged yellow-cedar with phenol-resorcinol adhesive and hydroxymethylated resorcinol coupling agent. For Prod J 48:81

Pivsa-Art W, Fujii K, Nomura K, Aso Y et al (2016) The effect of poly(ethylene glycol) as plasticizer in blends of poly(lactic acid) and poly(butylene succinate). J Appl Polym Sci. https://doi.org/10.1002/app.43044

Rasche M (2012) Handbuch Klebtechnik (München [u.a.]: Hanser: München [u.a.]), https://doi.org/10.3139/9783446431980.fm

Sanchez-Ferrer A, Engelhardt M, Richter K (2023) Anisotropic wood-water interactions determined by dynamic vapor sorption: diffusivity and permeability. Cellulose 30:3869–3885. https://doi.org/10.1007/s10570-023-05093-z

Schneider A (1969) Contributions on the dimensional stabilization of wood with polyethylene glycole - part1: basic investigations on the dimensional stabilization of wood with polyethylene glycol. Holz Roh- Werkst 27:209–224. https://doi.org/10.1007/BF02612917

Schneider A (1970) Contributions on the dimensional stabilization of wood with polyethylene glycole - part 2: investigations on changes of wood properties by PEG impregnation and on the effectiveness of various impregnation processes. Holz Roh- Werkst 28:20–34. https://doi.org/10.1007/BF02615722

Schneider A (1977) Evaluation criteria for the effectiveness of the dimensional stabilization of the wood through the incorporation of bulky substances in the cell wall. Holz Roh- Werkst 35:213–217. https://doi.org/10.1007/BF02608335

Sing KSW, Everett DH, Haul RAW, Moscou L et al (1985) Reporting physisorption data for gas/solid systems with special reference to the determination of surface area and porosity (Recommendations 1984). Pure Appl Chem 57:603–619. https://doi.org/10.1351/pac198557040603

Son J, Tze WT, Gardner DJ (2005) Thermal behavior of hydroxymethylated resorcinol (HMR)-treated maple veneer. Wood Fiber Sci 37:220–231

Stamm AJ (1956) Dimensional stabilization of wood with carbowayes. For Prod J 6:201–204

Stamm AJ (1959) Effect of polyethylene glycol on the dimensional stability of wood. For Prod J 9:375–381

Sun N, Frazier CE (2005) Probing the hydroxymethylated resorcinol coupling mechanism with stress relaxation. Wood Fiber Sci 37:673–681

Swiezkowski F, Dolan P, Amen-Chen C, Gabriel J (2017) Adhesive system for preparing lignocellulosic composites. U.S. Patent No. 9,649,826, U.S. Patent and Trademark Office

Tarkow H, Feist W, Southerland C (1966) Interaction of wood with polymeric materials: penetration versus molecular size. For Prod J 16:61–65

Vick CB, Richter K, River BH, Fried ARJ (1995) Hydroxymethylated resorcinol coupling agent for enhanced durability of bisphenol-A-epoxy bonds to sitka spruce. Wood Fiber Sci 27:2–12

Viollaz PE, Rovedo CO (1999) Equilibrium sorption isotherms and thermodynamic properties of starch and gluten. J Food Eng 40:287–292. https://doi.org/10.1016/S0260-8774(99)00066-7

Washburn EW (1921) The dynamics of capillary flow. Phys Rev 17:273–283. https://doi.org/10.1103/PhysRev.17.273

Willems W (2014) The water vapor sorption mechanism and its hysteresis in wood: the water/void mixture postulate. Wood Sci Technol 48:499–518. https://doi.org/10.1007/s00226-014-0617-4
Willems W (2015) A critical review of the multilayer sorption models and comparison with the sorption site occupancy (SSO) model for wood moisture sorption isotherm analysis. Holzforschung 69:67–75. https://doi.org/10.1515/hf-2014-0069
Wimmer R, Kläusler O, Niemz P (2013) Water sorption mechanisms of commercial wood adhesive films. Wood Sci Technol 47:763–775. https://doi.org/10.1007/s00226-013-0538-7
Yelle DJ, Ralph J (2016) Characterizing phenol–formaldehyde adhesive cure chemistry within the wood cell wall. Int J Adhes Adhes 70:26–36. https://doi.org/10.1016/j.ijadhadh.2016.05.002

Authors and Affiliations

Thomas Böger[1] · Max Engelhardt[1] · Francis Tangwa Suh[2] · Klaus Richter[1] · Antoni Sanchez-Ferrer[1]

✉ Thomas Böger
boeger@hfm.tum.de

✉ Antoni Sanchez-Ferrer
sanchez@hfm.tum.de

Max Engelhardt
engelhardt@hfm.tum.de

Francis Tangwa Suh
tangwasuh86@gmail.com

Klaus Richter
richter@hfm.tum.de

[1] Chair of Wood Science, School of Life Sciences, Technical University of Munich, Winzererstr. 45, 80797 Munich, Germany

[2] Rosenheim University of Applied Sciences, Rosenheim, Germany